PAPER *Special Section on Nonlinear Theory and Its Applications*

Chaotic Oscillators Derived from Saito's Double-Screw Hysteresis Oscillator

Ahmed S. ELWAKIL† *and* **Michael Peter KENNEDY**†, *Nonmembers*

SUMMARY The fact that there exists a core sinusoidal oscillator at the heart of Saito's double-screw hysteresis chaotic oscillator is demonstrated. By applying Bruton's transformation to the active linear part of the circuit, which is shown to be a classical LC-R negative resistor sinusoidal oscillator, an inductorless realization based on a frequency-dependent negative resistor (FDNR) is obtained. The LC-R sinusoidal oscillator is replaced by an FDNR-R oscillator. Furthermore, we show that chaotic behaviour can be preserved when a simple minimum component 2R-2C sinusoidal oscillator is used. Two different realizations of the non-monotone current-controlled hysteresis resistor, one of which is completely passive, are investigated. Experimental results of selected circuits, PSpice and numerical simulations are included.

key words: *chaos, oscillators, hysteresis, double-screw*

1. Introduction

A hysteretic chaotic oscillator is one in which the nonlinear element exhibits hysteretic behaviour resulting from slow-fast dynamics. Hysteretic behaviour in electronic circuits, such as that which occurs in a Schmitt trigger or a non-monotone nonlinear resistor, is normally associated with fold bifurcations; it manifests itself as "jumps" in voltages or currents at impasse points [1]. The fast dynamics associated with a non-monotone current-controlled (voltage-controlled) negative resistor may be modelled by a small transit inductance (capacitance) in series (parallel) with the resistor [1], [2]. Several hysteresis chaos generators have been introduced in literature [3]–[7] and most recently in [8], [9]. However, Saito's double-screw oscillator [6] has gained wide popularity as a classical hysteretic chaotic oscillator which has been modelled and analyzed in detail [6], [10]. This oscillator, shown in Fig. 1 (a), contains a non-monotone current-controlled hysteresis resistor N_R, an inductor L, a capacitor C, and a linear current-controlled negative resistor R, in addition to the transit inductance L_0 which completes the model. The linear negative resistor adds energy to the circuit to separate trajectories while the hysteresis element switches the trajectory between two dimensional regions to keep it bounded. A practical implementation of Saito's oscillator is shown in Fig. 1 (b) [6], [10]. The linear negative resistor is implemented by means of op amp U_1 and resistors R_1, R_2, R_3 whereas the hysteresis resistor is constructed using op amp U_2, resistors R_4, R_5, R_6 and two zener diodes. A typical hysteresis loop is shown in Fig. 1 (c) when $R_4 = R_5 = 10\,\mathrm{k\Omega}$, $R_6 = 5\,\mathrm{k\Omega}$ and using standard 3.3 V zener diodes.

It is the aim of this work to show that Saito's chaotic oscillator can be functionally decomposed into two directly coupled blocks, namely a sinusoidal oscillator and a current-controlled hysteresis resistor. First we consider two realizations of the hysteresis resistor

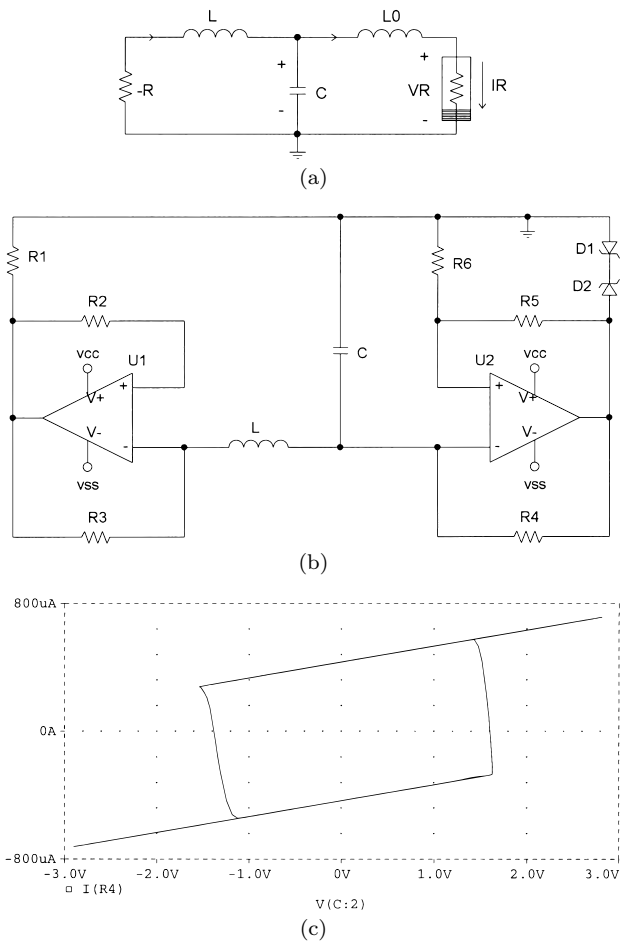

Fig. 1 (a) Saito's double-screw hysteresis oscillator, (b) Implementation given in [6], [10], (c) Typical hysteresis loop.

Manuscript received November 9, 1998.
Manuscript revised March 23, 1999.

†The authors are with the Department of Electronic and Electrical Engineering, University College Dublin, Dublin 4, Ireland.

different from the one shown in Fig. 1 (b) and confirm the observation of the double-screw using one of these realizations, which is active, and the single-screw using the other, which is passive. Next, we show that the linear active part of Saito's circuit is actually the classical LC-R sinusoidal oscillator. Hence, by applying Bruton's transformation [11], this oscillator can be replaced with an FDNR-R oscillator resulting in an inductorless realization of the chaotic circuit. This realization further inspires another chaotic oscillator based on a minimum component 2R-2C sinusoidal oscillator. In conclusion, two facts are stressed:

1) The stretching mechanism in Saito's oscillator is actually not performed by the linear negative resistor (see Fig. 1 (a)), but rather more generally with an active sinusoidal oscillator.
2) The folding mechanism is performed by a nonlinear resistor which is not necessarily active.

Experimental results, PSpice and numerical simulations are shown.

2. New Implementations of Saito's Oscillator

2.1 Using Different Nonlinear Resistors

Recently, a 4D chaotic oscillator based on a differential hysteresis comparator was proposed in [9]. From this oscillator, the differential hysteresis comparator is extracted, its single-ended form obtained and then employed as the current-controlled nonlinear resistor in Saito's oscillator. Due to its symmetry, the observation of a double-screw attractor is expected. The resulting realization of Saito's circuit is shown in Fig. 2 (a) where resistors R_2, R_3, R_4 and the associated op amps synthesize the hysteresis comparator. Note that the linear negative resistor is realized using a current feedback op amp (CFOA) and a single grounded resistor R_1. This realization requires two resistors less than a conventional realization based on a voltage op amp (VOA) and improves the circuit's frequency response [12], [13].

PSpice simulations of the circuit in Fig. 2 (a) were carried out using an AD844 CFOA, TL084 (AD713) VOAs, all biased with $\pm 9\,\mathrm{V}$ supplies, and taking $L = 100\,\mathrm{mH}$, $C = 4.7\,\mathrm{nF}$, $R_1 = 3\,\mathrm{k\Omega}$, $R_2 = 10\,\mathrm{k\Omega}$, $R_3 = 100\,\mathrm{k\Omega}$ and $R_4 = 12\,\mathrm{k\Omega}$. As expected, the double-screw chaotic attractor [6] is observed, as shown in Fig. 2 (b).

Consider optimizing this circuit for high-speed, low-voltage and low-power applications. It can be realized that the optimization process is not easy due to the active nature of the nonlinear resistor. Hence, we investigate the possibility of utilizing a passive S-shaped (current-controlled) negative differential resistor instead of the active hysteresis resistor. A catalogue of such nonlinear resistors using bipolar transistors has been introduced in [14]. From this catalogue, a simple two-transistor, one-resistor implementation is selected and incorporated into Saito's oscillator as shown in Fig. 3 (a). The S-shaped nonlinear resistor is composed of transistors Q_P and Q_N in addition to resistor R_2. Due to its antisymmetric current-voltage characteristics (experimental I–V characteristics for different values of R_2 are shown in Fig. 2 (b) of [14]), only a single-screw can be observed in the PSpice simulation (Fig. 3 (b)) of the circuit which is performed with $L = 47\,\mu\mathrm{H}$, $C = 47\,\mathrm{pF}$, $R_1 = 150\,\Omega$ and $R_2 = 2\,\mathrm{k\Omega}$. Here, a BC559 PNP transistor and a Q2N2222 NPN transistor were used. It is clear that chaotic behaviour persists when a passive nonlinear resistor is used, although only a single-screw is observed in this case. From a circuit design point of view, the operating frequency and power supply limitations imposed by a passive nonlinear resistor are mainly those dictated by the fabrication technology. Also, from an application point of view, there is no evidence that double-screw chaos is more advantageous than single-screw chaos. Hence, passive nonlinearities are recommended where possible.

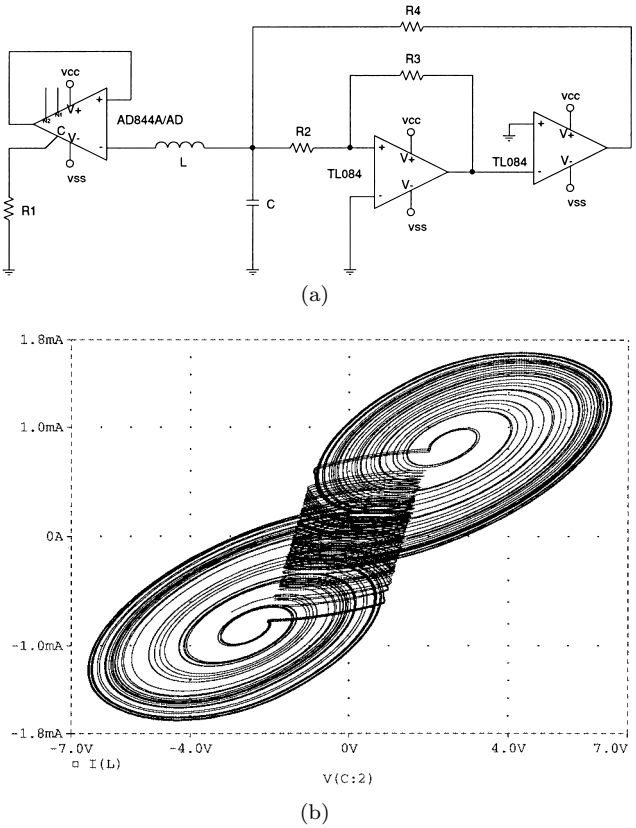

Fig. 2 (a) New realization of Saito's oscillator using a single-ended hysteresis comparator [9], (b) The obtained double-screw chaotic attractor in the V_C–I_L plane.

2.2 Inductorless Implementations Based on Saito's Circuit Decomposition

Although it is possible to obtain an inductorless re-

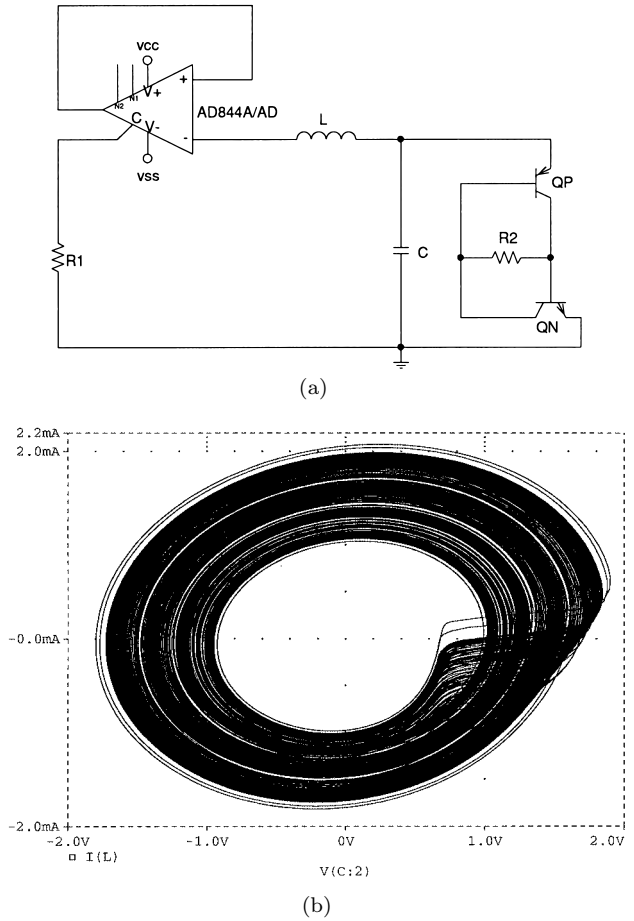

(a)

(b)

Fig. 3 (a) Saito's oscillator using a differential S-shaped passive nonlinear resistor, (b) The observed single-screw attractor in the V_C–I_L plane.

alization of Saito's oscillator by directly replacing the inductor with an active RC circuit that emulates its function, a different and more compact approach can be adopted based on physical decomposition of this circuit into two directly coupled blocks: a sinusoidal oscillator and a nonlinear resistor. This decomposition not only facilitates circuit realization but provides a different understanding of the stretching mechanism of the trajectories.

Consider the capacitor C shown in Fig. 1 (a). This capacitor can be thought of as composed of two parallel capacitors: a relatively large capacitor C_O and another smaller one C_S. It can thus be seen that the negative linear resistor along with the inductor and capacitor C_O form a classical active tank resonator, also known as the LC-R sinusoidal oscillator. The non-monotone resistor, the transit inductor L_0 and the switching capacitance C_S form the hysteresis resistor. C_S can practically be a parasitic capacitor. Accordingly, Bruton's transformation [11] can be applied to the LC_O-R oscillator resulting in the inductor being transformed into a resistor while C_O transforms into a frequency-dependent negative resistor (FDNR), which is a linear active block. Such an implementation is shown in Fig. 4 (a) where the components R_1, R_2, R_3, C_1, C_2 and the corresponding op amps form an FDNR based on Antoniou's classical GIC [15]. The grounded resistor R is the transformed inductor. The rest of the circuit represents the hysteresis resistor and the parasitic switching capacitor.

A PSpice simulation of the circuit was carried out taking $R_1 = R_2 = R_3 = 2.5\,\mathrm{k\Omega}$, $R_4 = R_5 = 10\,\mathrm{k\Omega}$, $R_6 = R = 5\,\mathrm{k\Omega}$, $C_1 = C_2 = 1\,\mathrm{nF}$, $C = 100\,\mathrm{pF}$ and using 3.3 V zener diodes. Indeed, the double-screw attractor is observed as shown in Fig. 4 (b). This behaviour persists with even smaller values of C. Thus the stretching mechanism in Saito's circuit is actually performed by a sinusoidal oscillator and not just by a linear negative resistor. This understanding agrees well with recent results of studying the dynamics of the chaotic Colpitts oscillator [16], [17] and Chua's circuit [18].

Since the active tank resonator and its FDNR-R transformation are nothing but sources of sinusoidal oscillations when disconnected from any nonlinear resistor, we investigate the possibility of using a minimum component 2R-2C sinusoidal oscillator to replace the active resonator. This results in the circuit shown in Fig. 5 (a) where the CFOA along with components R_1, R_2, C_1 and C_2 form a sinusoidal oscillator with a condition for oscillation and frequency of oscillation given respectively by:

$$\frac{R_1}{R_2} + \frac{C_2}{C_1} = 1 \quad \text{and} \quad \omega_0 = \frac{1}{\sqrt{R_2 C_2}} \tag{1}$$

A design set that satisfies the oscillation condition is to take $R_2 = 2R_1$ and $C_1 = 2C_2$. The ratio R_2/R_1 resembles a gain factor and should be slightly greater than 2 to start oscillations.

PSpice simulations of the circuit in Fig. 5 (a) were performed with $R_1 = 1\,\mathrm{k\Omega}$, $R_2 = 2.35\,\mathrm{k\Omega}$, $C_1 = 2\,\mathrm{nF}$, $C_2 = 1\,\mathrm{nF}$, $R_4 = R_5 = 10\,\mathrm{k\Omega}$ and $R_6 = 5\,\mathrm{k\Omega}$. The observed chaotic attractor in the V_{C2}–I_{R4} plane is shown in Fig. 5 (b). Note that the current I_{R4} is essentially the same current in the transit inductor L_0.

It is worth noting that although in the sinusoidal oscillator R_1 and C_1 can interchange positions without affecting its behaviour, this is not possible once coupled to the hysteresis resistor, since C_1 also plays the role of the switching capacitor, which is an essential part of Saito's oscillator.

The following equation set describes this chaotic oscillator:

$$\begin{aligned} C_1\dot{V}_{C1} &= \frac{V_{C2} - V_{C1}}{R_1} - I_{L0} \\ C_2\dot{V}_{C2} &= \left(\frac{1}{R_1} - \frac{1}{R_2}\right) V_{C2} - \frac{1}{R_1} V_{C1} \\ L_0 I_{L0} &= V_{C1} - V_R \end{aligned} \tag{2a}$$

and V_R is the voltage across the nonlinear resistor expressed as:

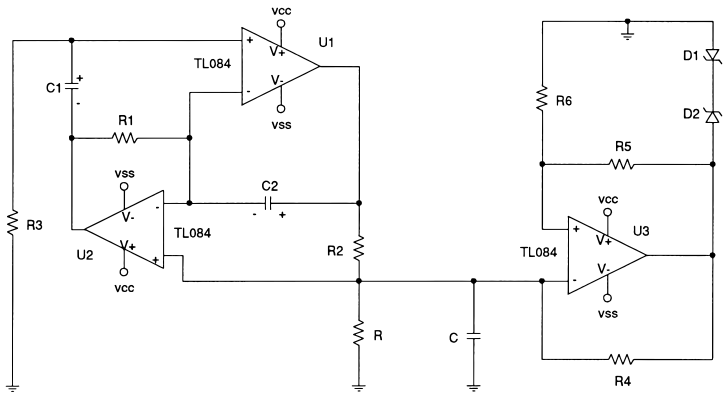

(a)

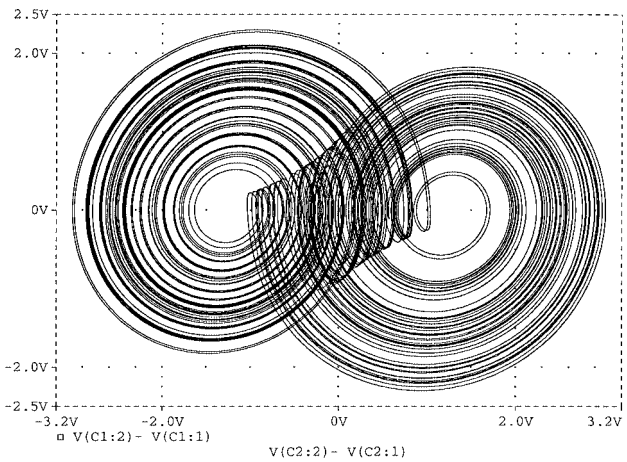

(b)

Fig. 4 (a) Inductorless realization of Saito's oscillator resulting from the application of Bruton's transformation to the active tank resonator, (b) The double-screw attractor in the V_{C1}–V_{C2} plane.

$$V_R = R_b I_{L0} + \frac{1}{2}(R_a - R_b)(|I_{L0} + I| - |I_{L0} - I|), \tag{2b}$$

where R_a and R_b are the slopes in the inner and outer regions respectively and $\pm I$ are the breakpoints [10]. For the choice of $C_1 = 2C_2 = 2C$, $R_2 = KR_1 = KR$ and by setting:

$$\tau = \frac{t}{RC},\ X = \frac{V_{C1}}{V_n},\ Y = \frac{V_{C2}}{V_n},\ Z = \frac{RI_{L0}}{V_n},$$
$$\alpha_1 = \frac{R_b}{R},\ \alpha_2 = \frac{1}{2}\frac{R_a - R_b}{R},\ \beta = \frac{R^2 C}{L_0},\ m = \frac{RI}{V_n},$$

where V_n is an arbitrary voltage normalization constant (=1 V), equation set (2) transforms into the following dimensionless form:

$$\begin{aligned} 2\dot{X} &= Y - X - Z \\ \dot{Y} &= \left(1 - \frac{1}{K}\right) Y - X \\ \dot{Z} &= \beta(X - f(Z)) \end{aligned} \tag{3a}$$

and

$$f(Z) = \alpha_1 Z + \alpha_2(|Z + m| - |Z - m|) \tag{3b}$$

Numerical integration of (3) was carried out using an adaptive-step Runge-Kutta algorithm taking $K = 2.5$, $\alpha_1 = 10$, $\alpha_2 = -7.5$, $m = 0.25$ and $\beta = 1000$. The nonlinear resistor parameters R_a, R_b and I were taken as: $-5\,\mathrm{k\Omega}$, $10\,\mathrm{k\Omega}$ and $250\,\mu\mathrm{A}$ respectively. The obtained X–Y–Z trajectory is plotted in Fig. 5 (c). Chaotic behaviour persists for a wide range of parameter values ($\beta \in [0.5, 1000]$, $K \in [2.25, 3.2]$, $\alpha_1 \in [3, 14]$, $\alpha_2 \in [-5, -25]$, $m \in [0.1, 10]$).

Using the same 2R-2C sinusoidal oscillator coupled to the passive S-shaped nonlinear resistor, as shown in Fig. 6 (a), a single screw can be observed. Figure 6 (b) shows a PSpice simulation carried out with $R_1 = 1\,\mathrm{k\Omega}$, $R_2 = 2.24\,\mathrm{k\Omega}$, $C_1 = 2\,\mathrm{nF}$, $C_2 = 1\,\mathrm{nF}$ and $R_3 = 2\,\mathrm{k\Omega}$. Note however, that the role of the switching capacitor is now performed by C_2 instead of C_1 as compared to Fig. 5 (a). The S-shaped nonlinear resistor possesses two turning points; a peak point (I_P, V_P) and a valley point (I_V, V_V) [14]. Thus the chaotic oscillator of Fig. 6 (a) can be described by the following equations:

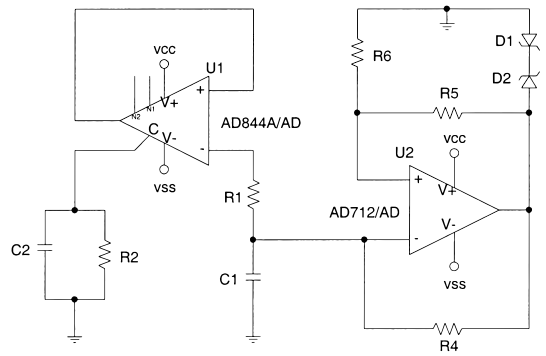

(a)

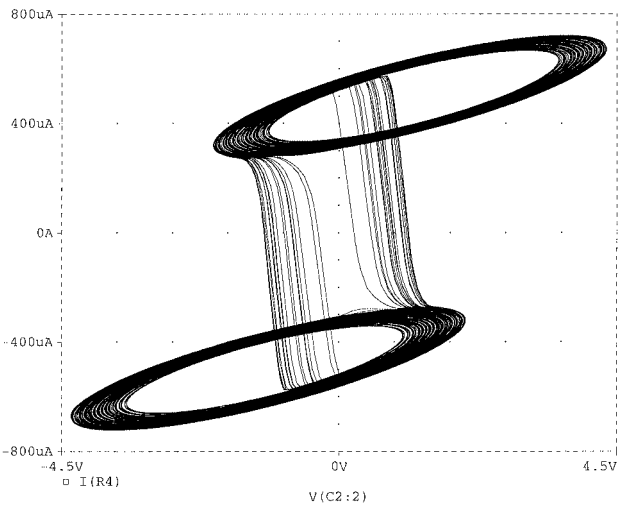

(b)

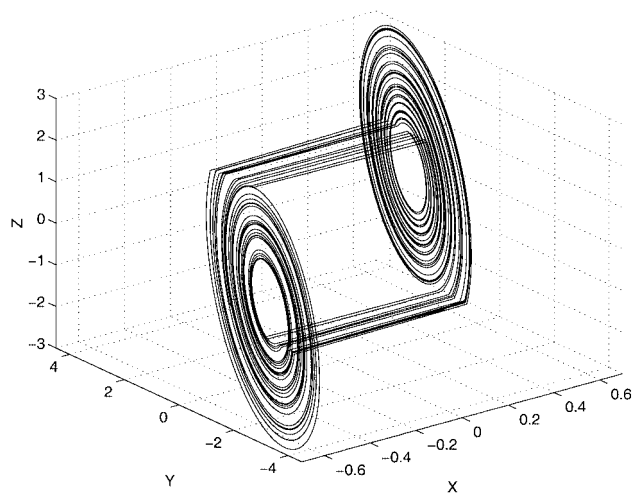

(c)

Fig. 5 (a) Derived chaotic oscillator based on a 2R-2C sinusoidal oscillator and using the active hysteresis resistor, (b) Observed attractor in the V_{C2}–I_{R4} plane, (c) The X–Y–Z phase space trajectory obtained by numerically integrating (3).

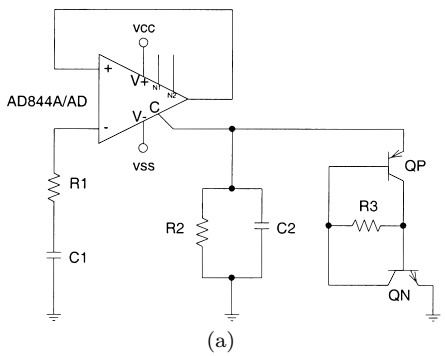

(a)

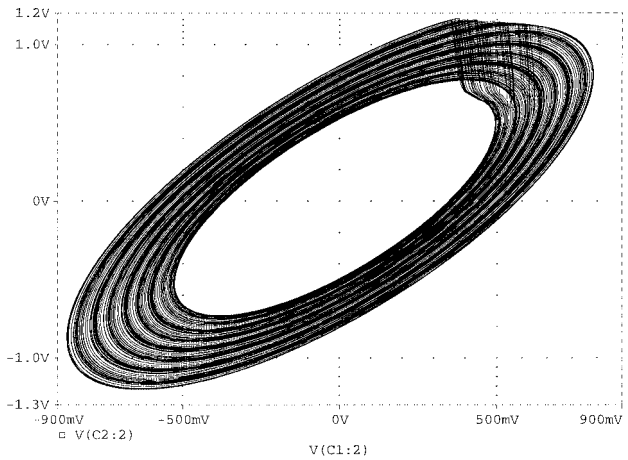

(b)

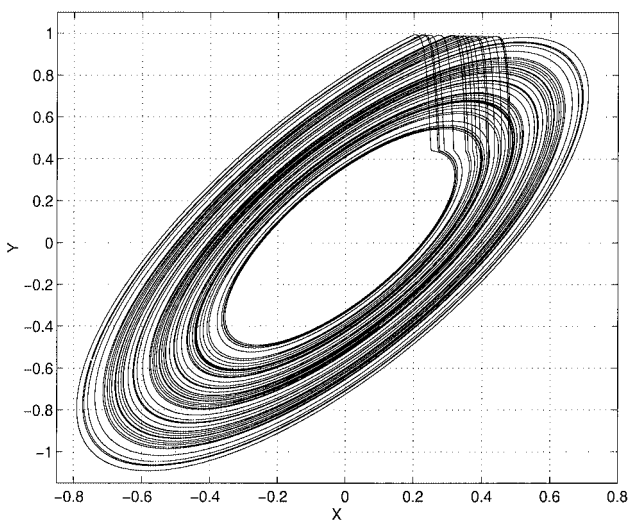

(c)

Fig. 6 (a) Derived chaotic oscillator based on a 2R-2C sinusoidal oscillator and using a passive S-shaped nonlinear resistor, (b) Observed single-screw attractor in the V_{C1}–V_{C2} plane, (c) X–Y trajectory obtained from numerical integration of (5).

$$
\begin{aligned}
C_1\dot{V}_{C1} &= \frac{V_{C2}-V_{C1}}{R_1} \\
C_2\dot{V}_{C2} &= \left(\frac{1}{R_1}-\frac{1}{R_2}\right)V_{C2}-\frac{1}{R_1}V_{C1}-I_{L0} \qquad (4a)\\
L_0\dot{I}_{L0} &= V_{C2}-V_R
\end{aligned}
$$

and V_R is the voltage across the nonlinear resistor expressed as:

$$
V_R=\begin{cases}
\dfrac{I_{L0}}{I_V} & I_{L0}\geq I_V \\
V_P-\dfrac{V_P-V_V}{I_V-I_P}(I_{L0}-I_P) & I_P\leq I_{L0}<I_V \\
\dfrac{V_P}{I_P}I_{L0} & 0\leq I_{L0}<I_P
\end{cases} \qquad (4b)
$$

With the same expressions of X, Y, Z, τ and β used to derive (3) in addition to the following settings:

$$
P_1=\frac{V_P}{V_V}, P_2=\frac{I_V}{I_P}, V_{V_n}=\frac{V_V}{V_n}, m=\frac{RI_V}{V_n},
$$

the dimensionless form of (4) is given by:

$$
\begin{aligned}
2\dot{X} &= Y-X \\
\dot{Y} &= \left(1-\frac{1}{K}\right)Y-X-Z \qquad (5a)\\
\dot{Z} &= \beta(Y-f(Z)) \quad \text{and}
\end{aligned}
$$

$$
f(Z)=V_{V_n}\begin{cases}
\dfrac{Z}{m} & Z\geq m \\
P_1-\dfrac{P_1-1}{P_2-1}\left(\dfrac{P_2}{m}Z-1\right) & \dfrac{m}{P_2}\leq Z<m \\
\dfrac{P_1P_2}{m}Z & 0\leq Z\dfrac{m}{P_2}
\end{cases} \qquad (5b)
$$

Numerical integration of (5) was carried out using an adaptive-step Runge-Kutta algorithm taking $K=2.4$, $P_1=1.56$, $P_2=100$, $m=5$, $V_{V_n}=0.63$ and $\beta=1000$. The observed X–Y trajectory is shown in Fig. 6 (c).

3. Experimental Results

The circuits of Figs. 5 (a) and 6 (a) were verified experimentally with the same values used in PSpice simulations and taking R_2 as a 5 kΩ potentiometer for tuning. The V_{C2}–V_{R4} trajectory (V_{R4} is the voltage across R_4 measured by a differential probe) observed from the first circuit is shown in Fig. 7 (a). The results agree qualitatively with both PSpice and numerical simulations. Figure 7 (b) represents the V_{C1}–V_{C2} trajectory of the second circuit which was implemented with a BC559 PNP transistor and a Q2N2222 NPN transistor. The results are also in good agreement with PSpice and numerical simulations. The measured power dissipation of the circuit in Fig. 5 (a) was found

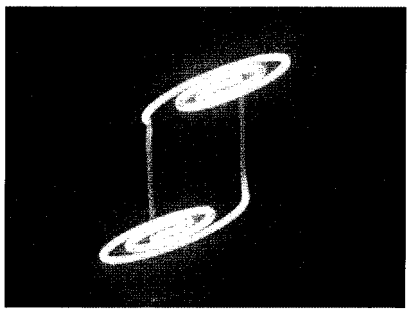

(a)

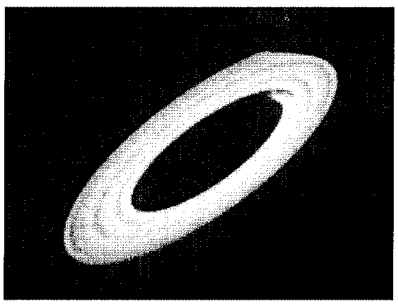

(b)

Fig. 7 (a) Experimental results of the circuit in Fig. 5 (a). Xaxis: V_{C2} 0.1 V/div, Yaxis: V_{R4} 1 V/div. (b) Experimental results of the circuit in Fig. 6 (a). Xaxis: V_{C1} 0.2 V/div, Yaxis: V_{C2} 0.2 V/div.

to be 830 mW while it was 108 mW for the circuit in Fig. 6 (a). Both circuits used ±9 V supplies. The measured power reduction ratio (P_{rr}) is thus $P_{rr}=7.7$. This is due to the antisymmetric characteristics of the passive nonlinear resistor which allows a current swing of approximately 6 mA while the active nonlinear resistor employs an op amp with a current swing of approximately 60 mA. We confirm this observation by calculating a power dissipation figure from the mathematical models of (3) and (5) respectively. The quantity $Q=\dfrac{1}{T}\displaystyle\int_0^T (X(t)^2+Y(t)^2+Z(t)^2)dt$, with a sufficiently long simulation period T, is a good measure of the average power consumption. For $T=300$, integration of (3) results in $Q=4.94$ while (5) results in $Q=0.51$. We calculate $P_{rr}=9.7$, which is in acceptable agreement with experimental observations.

4. Conclusions

We emphasize the fact that chaotic behaviour is associated with the functions performed by groups of elements rather than by individual components. This was demonstrated on the linear active part of Saito's chaotic oscillator, which is essentially an LC-R sinusoidal oscillator, where it was shown that other sinusoidal oscillator circuits can lead to chaotic behaviour as well. It is thus beneficial to develop a functional model of any chaotic oscillator first by separating the linear and

nonlinear parts from each other and then by describing the function performed by each part. In conclusion we stress the following two points:

1) The stretching mechanism in Saito's oscillator is actually not performed by the linear negative resistor (see Fig. 1 (a)), but rather more generally by an active sinusoidal oscillator. In this sense, inductorless realizations are directly obtained by using an RC sinusoidal oscillator.
2) The folding mechanism is performed by a nonlinear resistor which is not necessarily active.

References

[1] M.P. Kennedy and L.O. Chua, "Hysteresis in electronic circuits: A circuit theorist's perspective," Int. J. Circuit Theory & Applications, vol.19, pp.471–515, 1991.
[2] L.O. Chua and P.M. Lin, Computer-aided analysis of electronic circuits: Algorithms and computational techniques, Prentice-Hall, Englewood Cliffs, New Jersey, 1975
[3] P.W. Newcomb and S. Saythan, "An RC op amp chaos generator," IEEE Trans. Circuits & Syst.-I, vol.30, pp.54–56, 1983.
[4] T. Saito, 'An approach towards higher dimensional hysteresis chaos generators," IEEE Trans. Circuits & Syst.-I, vol.37, pp.399–409, 1990.
[5] K. Kohari, T. Saito, and H. Kawakami, "On a hysteresis oscillator including periodic thresholds," IEICE Trans. Fundamentals, vol.E76-A, no.12, pp.2102–2107, Dec. 1993.
[6] T. Saito and S. Nakagawa, "Chaos from a hysteresis and switched circuit," Phil. Trans. Royal Soc., vol.353, pp.47–57, 1995.
[7] S. Nakagawa and T. Saito, "An RC OTA hysteresis chaos generator," IEEE Trans. Circuits & Syst.-I, vol.43, pp.1019–1012, 1996.
[8] M. Storace and M. Parodi, "Simple realization of hysteresis chaos generator," Electron. Lett., vol.34, pp.10–11, 1998.
[9] J.E. Varrientos and E. Sanchez-Sinencio, "A 4D chaotic oscillator based on a differential hysteresis comparator," IEEE Trans. Circuits & Syst.-I, vol.45, pp.1–10, 1998.
[10] M.P. Kennedy, "Chaotic Circuit Behavior," Encyclopedia of Electrical and Electronics Engineering, vol.3, pp.226–241, Wiley, 1999.
[11] L.T. Bruton, "Network transfer functions using the concept of frequency-dependant negative-resistance," IEEE Trans. Circuit Theory, vol.16, no.3, pp.406–408, Aug. 1969.
[12] A.M. Soliman, "Applications of the current feedback operational amplifiers," Analog Integrated Circuits & Signal Processing, vol.14, pp.265–302, 1996.
[13] J. Bales, "A low power, high speed, current feedback op amp with a novel class AB high current output stage," IEEE J. Solid-State Circuits, vol.32, pp.1470–1474, 1997.
[14] L.O. Chua, J. Yu, and Y. Yu, "Negative resistance devices," Int. J. Circuit Theory & Applications, vol.11, pp.161–185, 1983.
[15] A. Antoniou, "Realization of gyrators using operational amplifier," Electron. Lett., vol.3, pp.350–352, 1967.
[16] M.P. Kennedy, "Chaos in the Colpitts oscillator," IEEE Trans. Circuits & Syst.-I, vol.41, pp.771–774, 1994.
[17] G.M. Maggio, O. De Feo, and M.P. Kennedy, "Nonlinear analysis of the Colpitts oscillator and applications to design," IEEE Trans. Circuits & Syst.-I, vol.46, no.9, Sept. 1999.
[18] A.S. Elwakil and M.P. Kennedy, "Chua's circuit decomposition: A sinusoidal oscillator coupled to an active voltage controlled nonlinear resistor," submitted to Int. J. Circuit Theory Appl.

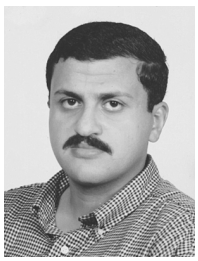

Ahmed S. Elwakil was born in Cairo, Egypt in 1972. He received his B.Sc. and M.Sc. degrees from the Department of Electronics and Communications, Faculty of Engineering, Cairo University in 1995 and 1997 respectively. After graduation, he joined the staff at the Egyptian Nuclear Research Center. In 1997, he was offered a Ph.D. scholarship from the National University of Ireland (University College Dublin) where he is currently carrying out research in the area of nonlinear dynamics and chaos generation. He is author and co-author of more than 25 journal publications mostly reporting novel designs of harmonic and chaotic oscillators.

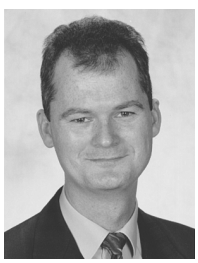

Michael Peter Kennedy received the B.E. (Electronic) degree from University College Dublin in 1984, and the M.S. and Ph.D. degrees in electrical engineering from the University of California at Berkeley in 1987 and 1991, respectively. Since 1992, he has been with the Department of Electronic and Electrical Engineering, University College Dublin, where he is an Associate Professor. His current research interests include chaotic communications, the design of chaotic oscillators, synchronization and control of chaos, and mixed-signal testing. Dr. Kennedy is a Fellow of the IEEE.